

KOSZALIN UNIVERSITY OF TECHNOLOGY

**RESEARCH AND MODELLING
IN CIVIL ENGINEERING
2018**

Edited by
Jacek Katzer, Krzysztof Cichocki and Jacek Domski

KOSZALIN 2018

MONOGRAPH NO 355
FACULTY OF CIVIL ENGINEERING,
ENVIRONMENTAL AND GEODETIC SCIENCES

ISSN 0239-7129
ISBN 978-83-7365-502-7

Chairman of the University Editorial Board
Zbigniew Danielewicz

Editors
Jacek Katzer, Krzysztof Cichocki and Jacek Domski
Koszalin University of Technology, Poland

Reviewers
Jacek Gołaszewski – Silesian University of Technology, Poland
Wojciech Sumelka – Poznań University of Technology, Poland

Technical editor
Czesław Suchocki

Website editor
Mariusz Ruchwa

Linguistic consultations
Ewa Sokółowska-Katzer

Typesetting
Czesław Suchocki

Cover design
Tadeusz Walczak

www.cecem.eu

© Copyright by Koszalin University of Technology Publishing House
Koszalin 2018

KOSZALIN UNIVERSITY OF TECHNOLOGY PUBLISHING HOUSE
75-620 Koszalin, Raławicka 15-17, Poland

Koszalin 2018, 1st edition, publisher's sheet 13,42, circulation 120 copies
Printing: INTRO-DRUK, Koszalin, Poland

Table of contents

1. Relationship between mechanical properties and conductivity of SCC mixtures with steel fibres	7
2. Quantitative comparison between visual and UAV-based inspections for the assessment of the technical condition of building facades	19
3. Choice of optimal material solutions for the assessment of heat and humidity states of outer walls made using the technology of light steel framing	31
4. Behaviour of high performance concrete in mixed mode loadings: experiments and numerical simulation	45
5. Performance and optimization of prestressed beam with respect to shape dimensions.....	63
6. Plate strip in a stabilized temperature field and creep effect	87
7. Harnessing digital image correlation system for assessing flexural characteristics of SFRC based on waste ceramic aggregate.....	113
8. An experimental analysis of the determination of the elastic modulus of cementitious materials.....	129
9. X-ray investigation of steel fibres in high performance self-compacting concrete beams	149
10. Binary alkali-activated materials with brick powder.....	171
11. Numerical analysis of the temperature distribution in an office room	187
12. Generalized maximum tangential stress criterion in double cantilever beam specimens: choice of the proper critical distance	199
13. Comparison of pulse-echo-methods for testing of heat degradation concrete	213
14. Fundamental formulae for the calculation of shear flexible rod structures and some applications	237

4. Behaviour of high performance concrete in mixed mode loadings: experiments and numerical simulation

Stanislav Seitl¹, Petr Miarka¹, Vlastimil Bílek², Wouter De Corte³

¹ *Brno University of Technology, Faculty of Civil Engineering, Brno, Czech Republic, orcid.org/0000-0002-4953-4324, orcid.org/0000-0002-4103-8617*

² *VŠB-Technical University of Ostrava, Faculty of Civil Engineering, Ostrava, Czech Republic, orcid.org/0000-0001-6433-4892*

³ *Ghent University, Faculty of Engineering and Architecture
Department of Structural engineering, Ghent, Belgium*

Abstract: The paper presents experimental and numerical results of HP concrete. Brazilian disc test is used in the evaluation of the fracture mechanical parameters.

Keywords: high performance concrete, numerical simulation, Brazilian disc

4.1. Introduction

The design of concrete structural elements used in civil engineering is optimized to reduce material consumption and to improve structural behavior. Concrete structures such as highway bridges, power plant cooling towers, shell roofs and especially prestressed concrete precast elements constitute important infrastructure and therefore receive increased attention in both design and subsequent maintenance. If well-organized, the use of precast concrete structural elements decreases construction time by two to three times in comparison to the traditional cast-in-place approach (Tomek R. 2017). The main requirement of investors in civil engineering is to extend the structural service life time by repair instead of complete replacement of the structure. The need for repair works is mainly caused by chemical actions of the environment or the long-term actions of load (i.e. creep). The other important global requirement is that the repair and construction must be environmentally friendly. This demand drives the development and use of new and advanced materials with reduced CO₂ consumption. This is also applicable to structures currently under construction and planned for the near future. (de Freitas V.P. 2013).

The prior renovation durability and sustainability of structures made from cementitious materials are often investigated in order to prevent accidents, unnecessary expenses and to get a basic understanding of the material used. To obtain a material sample from renovated structure, a core-drill is used to remove a cylindrical sample from the structure. The concrete samples are submitted for laboratory tests to identify the material's characteristics. The common material characteristics determined through testing the cylindrical specimen are: bulk density, the Young's modulus, the compressive strength, the flexural strength, etc. The design and structural behaviour of the abovementioned structures are, in the most cases, advanced and complex. These structures are not only subject to uniaxial load (tensile load), but very often to a combination of bending and tensile load (mixed mode I/II) conditions. To perform a modern advanced analysis of structural behaviour, knowledge of the material's fracture mechanical parameters is essential.

The advanced structural analysis uses fracture mechanical properties as an input parameter to predict total structural service life time and fracture resistance. The fracture parameters used in the advanced design are fracture toughness K_{IC} and fracture energy G_f . The structural elements after certain time can show minor surface damage or shrinkage can create micro-cracks. These defects are zones of weakness, where the crack can initiate. (Karihaloo B.L. 1995).

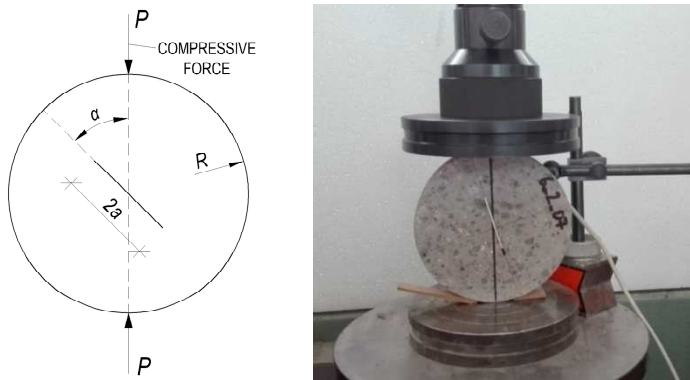


Fig. 4.1. Brazilian disc with central notch (left) and experimental setup (right).

The load presence on the structural element can be characterized by tensile mode I and shear mode II. In reality, some cracks are loaded by a combination of tension and shear - mixed mode I/II load. Hence, it is necessary to test material under the mixed mode loading conditions with circular cross section. The Brazilian disc test with a central notch (BDCN) suggests such application.

This contribution evaluates the fracture mechanical parameters of C 50/60 concrete material by the BDCN test specimen and investigates the failure and crack propagation process by employing the concrete damaged plasticity (CDP) material model. The fracture resistance curves were evaluated based on the maximum tangential stress (MTS) criterion (Erdogan F. and Sih G.C. 1963) and generalised maximum tangential stress (GMTS) criterion (Smith D. J. 2001). The MTS and GMTS criteria are commonly used for prediction of onset of fracture under the mode I, mixed mode I/II and mode II load conditions.

4.2. Material C 50/60

In this study, the investigated material was a C 50/60 concrete according to EN 206–1 (2005). In order to assess fracture mechanical properties and the FE numerical model, a C 50/60 was chosen because it is a typical material used for the pre-stressed precast elements, which are produced nowadays. C 50/60 shows variety in structural applications because of its high compressive and tensile strength. Usually, concrete with a compressive strength higher than 60 MPa and water to cement ratio lower than 0.42 can be considered as a high-performance concrete (HPC) (Nawy, E.G. 2001).

The mixture contains crushed high-quality granite 4/8 mm and 8/16 mm coarse aggregates and natural sand as a fine aggregate 0/4 mm. The water to cement ratio w/c was 0.4 and a polycarboxylates-based superplasticizer was used to reach good workability. The concrete was mixed in a volume of 1 m³, poured into moulds and tested at 28 days. Cone flow was measured 540 mm in accordance with (EN 12350-5 2009) and can be classified as class F4. Table 4.1 gives an overview of the material's mechanical properties.

Table 4.1. Overview of the mechanical properties of C 50/60 concrete at 28 days from Seitl et al. (2018) (mean values and standard deviation)

Young's Modulus E [GPa]	Bulk density ρ [kg/m ³]	Compressive cube strength f_{c_cube} [MPa]	Compressive cylindrical strength f_{c_cyl} [MPa]	Indirect tensile strength f_t [MPa]
38.3 ± 0.3	2390 ± 27.32	85.8 ± 2.9	72.8 ± 2.5	5.515 ± 0.31

To simulate proper material behaviour a nonlinear material model was used. The input parameters are based on the material stress-strain relation from CEB-FIP (Model Code 2010), which were evaluated from the experiments. To obtain a post peak behaviour (softening branch), damage parameters d_c for compression and d_t for tension were used. The maximum value of the tension damage parameter d_t was 0.99.

The recommendation provides a post peak behaviour in compression as well as in tension. It assumes a linear compressive behaviour up to 40% of the mean compressive strength f_{cm} , and after this point a quadratic function is used, which can be characterized by eq. 4.1.

$$\frac{\sigma_c}{f_{cm}} = - \left(\frac{k \cdot \eta - \eta^2}{1 + (k-2) \cdot \eta} \right) \text{ for } |\varepsilon_c| < |\varepsilon_{c,lim}| \quad (4.1)$$

where:

- f_{cm} – mean compressive strength,
- ε_{c1} – compressive strain at maximum compressive stress,
- $\varepsilon_{c,lim}$ – ultimate compressive strain,
- k – the plasticity number,
- η – $\eta = \varepsilon_c / \varepsilon_{c1}$

For a cracked section under tension, a bilinear stress-crack opening relation approach is used. The bilinear response can be characterized by eq. 4.2 and 4.3.

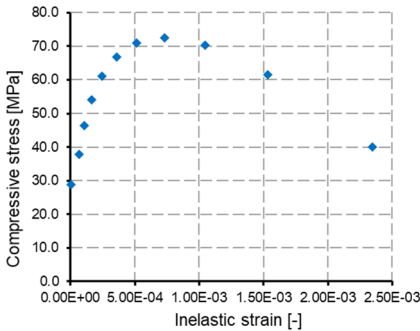
$$\sigma_{ct} = f_{cm} \left(1 - 0.8 \frac{w}{w_1} \right) \text{ for } w \leq w_1 \quad (4.2)$$

$$\sigma_{ct} = f_{cm} \left(0.25 - 0.05 \frac{w}{w_1} \right) \text{ for } w_1 < w \leq w_c \quad (4.3)$$

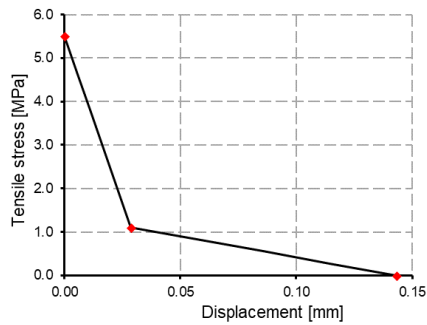
$$w_1 = \frac{G_f}{f_{ctm}} \text{ when } \sigma_t = 0.2 \cdot f_{ctm} ; w_c = \frac{5G_f}{f_{ctm}} \text{ when } \sigma_t = 0 \quad (4.4)$$

where:

- f_{ctm} – tensile strength,
- w – crack opening,
- $\varepsilon_{c,lim}$ – ultimate compressive strain,
- G_f – fracture energy $G_f = 73 \cdot f_{cm}^{0.18}$.
- w_1, w_c – limit points by eq. 4.4



(a)



(b)

Fig. 4.2. Input parameters for CDP material model - compression (a) and tension (b).

A material with similar mechanical and fracture mechanical properties was tested earlier by Zimmermann, T. and Lehký, D. (2015)

4.3. Theoretical Background

This contribution is based on a linear elastic fracture mechanics (LEFM). The LEFM uses for description of the stress field in the vicinity of a crack tip infinite power series, often called as a Williams expansion (Williams, M.L. 1956). The stress field description can be then described by a eq. 4.5.

$$\sigma_{i,j} = \frac{K_I}{\sqrt{2\pi r}} f_{i,j}^I(\theta) + \frac{K_{II}}{\sqrt{2\pi r}} f_{i,j}^{II}(\theta) + T + O_{i,j}(r, \theta), \quad (4.5)$$

where:

- $\sigma_{i,j}$ – stress tensor components,
- K_I – stress intensity factor for mode I,
- K_{II} – stress intensity factor for mode II,
- $f_{i,j}^I(\theta)$ – shape functions for mode I,
- $f_{i,j}^{II}(\theta)$ – shape functions for mode II,
- T – the second independent term on r ,
- O_{ij} – higher order terms
- r, θ – polar coordinates (with origin at the crack tip; crack faces lie along the x -axis)

According to the GMTS criterion (Smith, D.J. *et. al* 2001) the brittle fracture takes place radially from the crack tip and perpendicular to the direction of maximum tangential stress $\sigma_{\theta\theta}$. Crack growth initiates, when the $\sigma_{\theta\theta}$ reaches its maximum (critical value) $\sigma_{\theta\theta C}$. The $\sigma_{\theta\theta C}$ is reached under the crack initiation angle θ_0 and a critical distance from the crack tip r_C . Both θ_0 and r_C are material constants. The tangential stress $\sigma_{\theta\theta}$ around the crack tip can be expressed as:

$$\sigma_{\theta\theta} = \frac{1}{\sqrt{2\pi r}} \cos \frac{\theta}{2} \left[K_I \cos^2 \frac{\theta}{2} - \frac{3}{2} K_{II} \sin \theta \right] + T \sin^2 \theta + O(r^{1/2}) \quad (4.6)$$

While the MTS criterion uses only first terms (SIFs), the GMTS uses two terms of Williams expansion (SIFs and T -stress) in the series for $\sigma_{\theta\theta}$. The higher order terms $O(r^{1/2})$ are often negligible near the crack tip. Singular terms K_I , K_{II} and the T -stress are considered in the further analysis. According to the first hypothesis of the GMTS criterion, the angle of maximum tangential stress θ_0 is determined from:

$$\frac{\partial \sigma_{\theta\theta}}{\partial \theta} \Big|_{\theta=\theta_0} = 0 \text{ and } \frac{\partial^2 \sigma_{\theta\theta}}{\partial^2 \theta} < 0 \quad (4.7)$$

This assumption leads into the following equation:

$$\left[K_I \sin \theta_0 + K_{II} (3 \cos \theta_0 - 1) \right] - \frac{16T}{3} \sqrt{2\pi r_C} \cos \theta_0 \sin \frac{\theta_0}{2} = 0 \quad (4.8)$$

Eq. 4.8 shows that the angle θ_0 of maximum tangential stress for any combination of modes I and II depends on K_I , K_{II} , T and r_c . The angle θ_0 determined from eq. 4.8 is then used to predict beginning of the mixed mode fracture. According to GMTS criterion, the brittle fracture occurs when:

$$\sigma_{\theta\theta}(r_c, \theta_0) = \sigma_{\theta\theta,c} \quad (4.9)$$

By substituting the initiation angle θ_0 from eq. 4.9 into eq. 4.7, one can derive:

$$\sqrt{2\pi r_c} \sigma_{\theta\theta,c} = \cos \frac{\theta_0}{2} \left[K_I \cos^2 \frac{\theta_0}{2} - \frac{3}{2} K_{II} \sin \theta_0 \right] + \sqrt{2\pi r_c} T \sin^2 \theta_0 \quad (4.10)$$

Eq. 4.6 can be used for calculation of fracture initiation for pure mode I, pure mode II and mixed mode I/II. Pure mode I fracture initiation appears when $K_I = K_{IC}$,

$K_{II} = 0$. and $\theta_0 = 0^\circ$, this assumption simplifies eq. 4.10 to:

$$\sqrt{2\pi r_c} \sigma_{\theta\theta,c} = K_{IC} \quad (4.11)$$

where K_{IC} is the fracture toughness for mode I. By substituting eq. 4.11 into eq. 4.10 a general equation for mixed mode fracture is obtained.

$$K_{IC} = \cos \frac{\theta_0}{2} \left[K_I \cos^2 \frac{\theta_0}{2} - \frac{3}{2} K_{II} \sin \theta_0 \right] + \sqrt{2\pi r_c} T \sin^2 \theta_0 \quad (4.12)$$

4.3.1. Application of the GMTS Criterion to BDCN Geometry

Fracture resistance for both modes is expressed by ratio K_I/K_{IC} and K_{II}/K_{IC} . This ratio is obtained from eq. 4.12 by dividing whole expression by K_I , K_{II} respectively. Fracture resistance for mode I can be expressed as:

$$\frac{K_{IC}}{K_I} = \cos \frac{\theta_0}{2} \left[\cos^2 \frac{\theta_0}{2} - \frac{3}{2} \frac{K_{II}}{K_I} \sin \theta_0 \right] + \sqrt{2\pi r_c} \frac{T}{K_I} \sin^2 \theta_0 \quad (4.13)$$

and for mode II:

$$\frac{K_{IC}}{K_{II}} = \cos \frac{\theta_0}{2} \left[\frac{K_I}{K_{II}} \cos^2 \frac{\theta_0}{2} - \frac{3}{2} \sin \theta_0 \right] + \sqrt{2\pi r_c} \frac{T}{K_{II}} \sin^2 \theta_0 \quad (4.14)$$

From both eq. 4.13 and eq. 4.14 it is noticeable, that the fracture resistance depends not only on the first and second terms of Williams expansion, but also on the critical distance r_c . Literature shows two different options for the calculation of the r_c considering various boundary conditions. For plane stress and plane strain boundary condition (Anderson, T.L. 2017) the critical distance can be calculated by eq. 4.15 and eq. 4.12, respectively.

$$r_c = \frac{1}{2\pi} \left(\frac{K_{IC}}{\sigma_t} \right)^2 - \text{plane stress}, \quad (4.15)$$

$$r_c = \frac{1}{6\pi} \left(\frac{K_{IC}}{\sigma_t} \right)^2 - \text{plane strain}. \quad (4.16)$$

The values of the SIFs for a finite specimen with a shape of BDCN and the polar angle $\theta = 0^\circ$ can be expressed in the following form by eqs. 17 and 18 (Fett, T 2001, Ayatollahi, M.R. and Aliha, M.R.M. 2008, Seitzl et al 2018):

$$K_I = \frac{P\sqrt{a}}{RB\sqrt{\pi}} \frac{1}{\sqrt{1-\frac{a}{R}}} Y_I(a/R, \alpha) \quad (4.17)$$

$$K_{II} = \frac{P\sqrt{a}}{RB\sqrt{\pi}} \frac{1}{\sqrt{1-\frac{a}{R}}} Y_{II}(a/R, \alpha), \quad (4.18)$$

where:

- P – compressive load,
- a – crack length,
- R – radius of the disc ($D/2$),
- B – disc thickness,
- α – initial notch inclination angle,
- $Y_I(a/R, \alpha)$, – dimensionless shape function for mode I,
- $Y_{II}(a/R, \alpha)$ – dimensionless shape function for mode II.

4.3.2. Numerical Model - Geometry

A numerical simulation was performed using the FE software Abaqus (Abaqus 2016). For this, a two-dimensional (2D) plane stress model was created, and meshed with a 4-node linear element (type CPS4). The basic element size was 1 mm with refinements around the notch tip of 0.25 mm.

The simulated BDC specimen had a radius of $R = 75$ mm, initial notch lengths $2a = 40$ mm and $2a = 60$ mm (the relative crack length $a/R = 0.26$ and 0.4), and inclination notch angles α of 0° , 5° , 10° , 15° , 20° , 25° and 27° . The numerical analysis was performed with a displacement controlled loading at the top point of the BDCN specimen. The total induced vertical displacement was $u_y = -0.1$ mm ($u_x = 0$ mm) over the pseudo time step. Adequate boundary conditions were added to prevent rigid body translations (See Fig. 4.3).

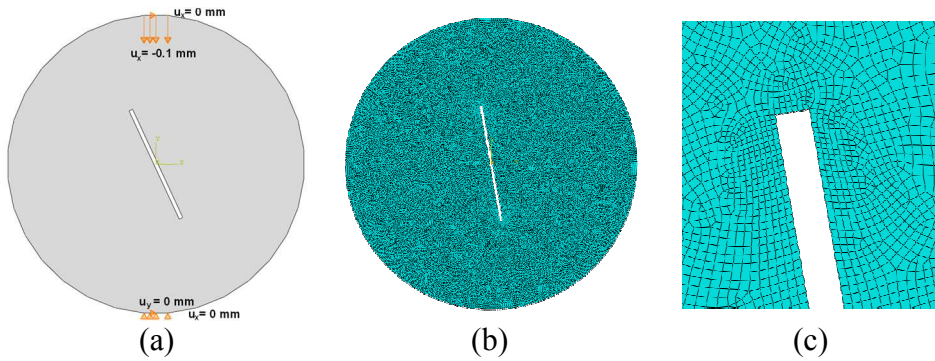


Fig. 4.3. Boundary conditions (left) and meshed BDC specimen with detail on the notch tip (right)

4.4.3. Material Model – Concrete Damaged Plasticity

The Concrete Damaged Plasticity (CDP) model was used similar like in Miarka, P. *et. al* (2018a). A brief introduction of the concrete damaged plasticity (CDP) material model, as implemented in (Abaqus 2016), is presented below. The model's yield function was proposed by Lubliner, J. *et. al* (1989) and later modified by Lee and Fenves Lee, J. and Fenves Gregory. L. (1998) to account for the different strength evolution in tension and compression. The yield function in terms of effective stresses has the following form:

$$F = \frac{1}{1-\alpha} (\bar{q} - 3\alpha\bar{p} + \beta(\bar{\varepsilon}^{pl})(\bar{\sigma}_{max}) - \gamma(-\bar{\sigma}_{max})), \quad (4.19)$$

where:

- \bar{p} – hydrostatic pressure,
- \bar{q} – von Misses equivalent effective stress,
- $\bar{\sigma}_{max}$ – maximum principal effective stress,
- α, β – constitutive parameters describing the flow of the yield function,
- γ – parameter related to the shape of the yield function,
- $Y_I(a/R, \alpha)$, – dimensionless shape function for mode I,
- $Y_{II}(a/R, \alpha)$ – dimensionless shape function for mode II,

Parameters α , β , and γ are expressed by eqs. 4.20 to 4.22.

$$\alpha = \frac{(\sigma_{b0}/\sigma_{c0})^{-1}}{2(\sigma_{b0}/\sigma_{c0})^{-1}-1}; 0 \leq \alpha \leq 0.5, \quad (4.20)$$

$$\beta = \frac{\sigma_c(\varepsilon_c^{pl})}{\sigma_t(\varepsilon_t^{pl})}(1 - \alpha) - (1 + \alpha), \quad (4.21)$$

where:

- σ_{b0} – biaxial compressive strength,
- σ_{c0} – uniaxial compressive strength,
- $\sigma_c(\varepsilon_c^{pl})$ – effective cohesion stresses for compression,
- $\sigma_t(\varepsilon_t^{pl})$ – the effective cohesion stresses for tension,

The shape of the yield surface is expressed as:

$$\gamma = \frac{3(1-K_c)}{2K_c-1}. \quad (4.22)$$

In this, K_c is the ratio of the tensile to the compressive meridian and defines the shape of the yield surface in the deviatoric plane in Fig. 4.4 (a). In biaxial compression, where $\bar{\sigma}_{max} = 0$, the parameter β is not active, and only the parameter α is being used. Parameter γ is active when the $\bar{\sigma}_{max} < 0$, which occurs in triaxial compression. The concrete damaged plasticity model uses the flow potential function $G(\sigma)$, which is a non-associated Drucker–Prager hyperbolic function and is defined by eq. 4.23.

$$G(\sigma) = \sqrt{(\varepsilon\sigma_{t0} \tan \psi)^2 + \bar{q}^2} - \bar{p} \tan \psi, \quad (4.33)$$

where:

- ε — eccentricity,
- ψ — dilation angle.

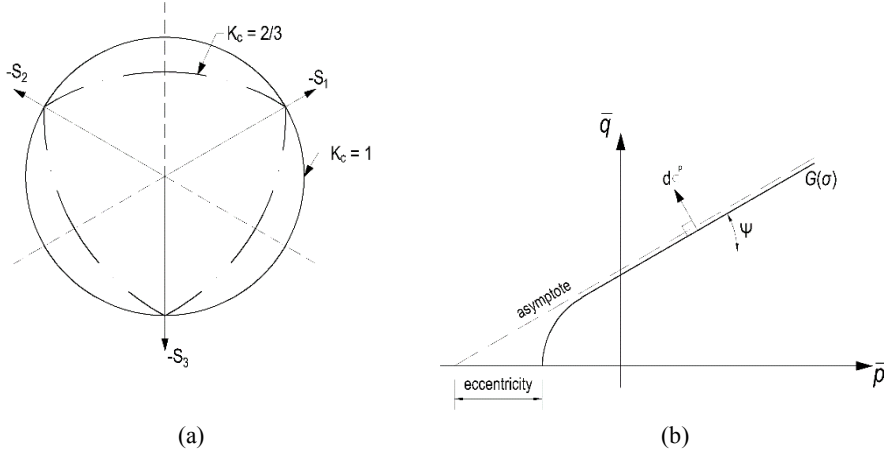


Fig. 4.4. Yield surfaces in the deviatoric plane ($K_c = 2/3$ corresponds to the Rankine formulation and 1 to the Drucker–Prager criterion) (a) and schematic of the plastic flow potential with dilation angle ψ and eccentricity in the meridian plane (b).

The CDP constitutive input parameters, which define the plasticity are shown in Table 4.2. These plasticity parameters were comprehensively studied by Kmiecik, P. And Kamiński, M. (2011) and showed accurate results.

Table 4.2. Input constitutive material parameters for CDP model.

Dilatation angle $\psi [^\circ]$	Eccentricity ε [-]	σ_{b0}/σ_{c0} [-]	K_c [-]	Viscosity parameter [-]
36	0.1	1.16	0.666	0

The CDP material model assumes that the uniaxial tensile and compressive response of concrete is characterized by damaged plasticity, which is defined by the damage parameter d and is used in the model according to Eq. (4.6).

$$\sigma = (1 - d)\bar{\sigma} = (1 - d)E_0(\varepsilon - \varepsilon^{pl}), \tag{4.24}$$

The damage parameter d is defined in terms of compression and tension d_c and d_t , respectively by:

$$(1 - d) = (1 - s_t d_c)(1 - s_c d_t), \tag{4.25}$$

where:

- s_t – tensile stiffness recovery,
 s_c – compressive stiffness recovery,

The damage parameters for compression d_c and tension d_t can be calculated according to Eq.(4.8) and Eq.(4.9), respectively

$$d_c = 1 - \frac{\sigma_c}{E_0(\varepsilon_c - \varepsilon_c^{pl})}, \quad (4.26)$$

$$d_t = 1 - \frac{\sigma_t}{E_0(\varepsilon_t - \varepsilon_t^{pl})}, \quad (4.27)$$

where:

- E_0 – tensile stiffness recovery,
 σ_c – compressive stress,
 σ_t – tensile stress,
 ε_c – compressive strain,
 ε_t – tensile strain,
 ε_c^{pl} – compressive plastic strain,
 ε_t^{pl} – tensile plastic strain,

3.4. Results and Discussion

An overview of fracture mechanical parameters of C 50/60 material and the numerical results from the FE simulations is given in next sections.

3.4.1. Mechanical - Fracture Properties

In total a series of 19 BDCN specimens were tested with a different a/R ratios and initial notch inclination angles α . The machine for tests has a maximum loading capacity 200 kN. The speed of the induced displacement of the upper support was equal to 0.025 mm/s.

A fracture toughness for mode I K_{IC} was evaluated from the test specimen with $\alpha = 0^\circ$ for both a/R ratios. The fracture toughness for mode II K_{IIC} were measured under the $\alpha = 27.7^\circ$ and $\alpha = 25.2^\circ$ for $a/R = 0.267$ and $a/R = 0.4$, respectively. The measured maximum forces for each inclination angle α and with evaluated stress intensity factors for both modes are presented in table 4.3.

Table 4.3. Overview of measured mean values of fracture loads P_c ($B=30$ mm), stress intensity factor for mode I K_I and mode II K_{II} for relative crack length $a/R = 0.267$ and 0.4 .

α [°]	a/R [-]	Load P_c [kN]	K_I [MPam ^{1/2}]	K_{II} [MPam ^{1/2}]
0	0.267	24.34	0.90	-
5		24.92	0.89	0.34
10		24.49	0.78	0.69
15		21.79	0.55	0.94
20		21.13	0.35	1.11
27.7		21.54	-	1.31
0	0.4	18.50	0.97	-
5		16.31	0.81	0.35
10		16.93	0.72	0.70
15		15.98	0.49	0.91
25.2		16.05	-	1.33

Fracture mechanical parameters evaluated from the BDCN test specimens are the fracture toughness for mode I K_{IC} and T -stress.

Table 4.4. Overview of measured fracture mechanical properties of C 50/60 material for $a/R = 0.267$ and 0.4 (Mean values and standard deviation).

Fracture toughness for mode I - K_{IC} [MPa m ^{1/2}]		T - stress [MPa]	
BDCN ($a/R = 0.267$)	BDCN ($a/R = 0.4$)	BDCN ($a/R = 0.267$)	BDCN ($a/R = 0.4$)
0.903 ± 0.09	0.973 ± 0.10	-13.92 ± 1.72	-12.13 ± 1.26

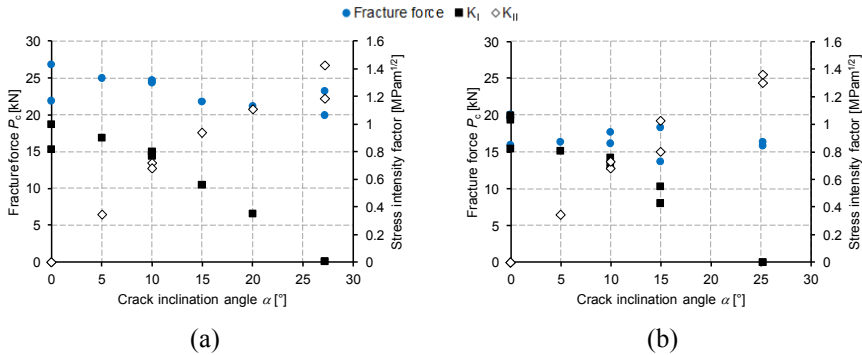


Fig. 4.5. Fracture forces and value of SIFs for selected angle α in case of relative notch length $a/R=0.267$ (a) and $a/R=0.4$ (b), respectively

From the knowledge of material fracture toughness and employing the MTS or the GMTS fracture criteria a material's fracture resistance curves can be evaluated. The fracture resistance curve curves evaluated for the C 50/60 concrete are show in Fig. 4.6.

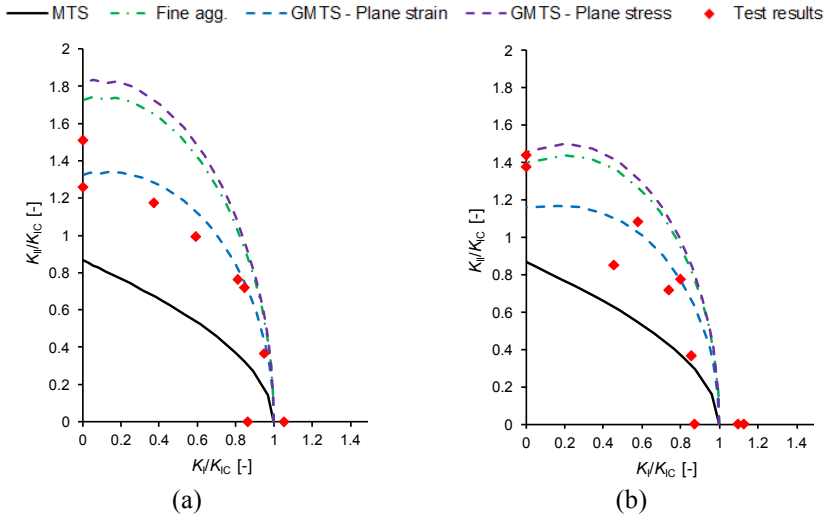


Fig. 4.6. Mixed mode I/II fracture resistance curves for C 50/60 for $a/R = 0.267$ (a) and $a/R=0.4$ (b).

The comparison of experimental results is done by fracture resistance curve. For each relative crack length, a/R and critical distance r_c were calculated resistance curves using eqs. 4.13 and 4.14. From Fig. 4.6, it can be noted, that the MTS criterion is very conservative (Seitl et. al 2018, Miarka et. al 2018). The GMTS criterion predict fracture resistance curves for both cases of a/R with good agreement especially for plane strain boundary condition for which the value of critical distance is $r_c = 1.559$ mm. For concrete the value of fracture process zone or (r_c) is relatively large in comparison with other engineering materials like polymers and metals, the effect of second term (T -stress) might not be ignored. For C 50/60 material, the critical distance r_c is 1.559 mm.

3.4.2. Numerical Results

Numerical software Abaqus generates a typical stress and inelastic strain fields for the studied geometry of the BDCN specimen. The inelastic strain represents smeared crack in the studied geometry. Stress and strain fields generated by numerical model give Figs 4.7-4.10 for each point of interest.

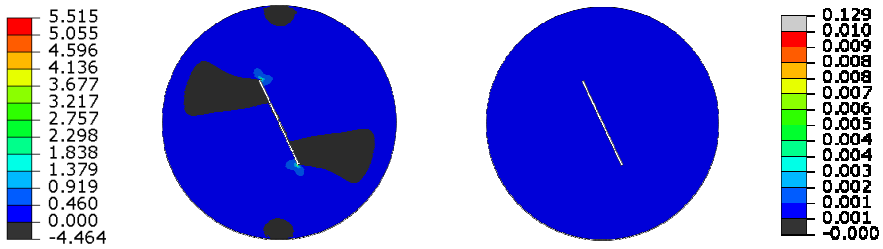


Fig. 4.7. Calculated maximum principal stress [MPa] and inelastic strain [-] fields with equivalent vertical compressive load for $a/R = 0.4$ and $\alpha = 25^\circ$, $P = 36.2$ N

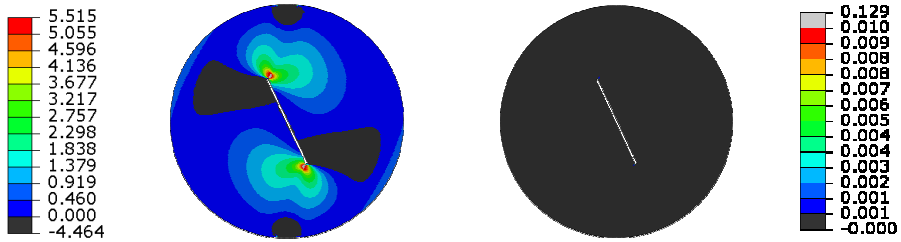


Fig. 4.8. Calculated maximum principal stress [MPa] and inelastic strain [-] fields with equivalent vertical compressive load for $a/R = 0.4$ and $\alpha = 25^\circ$, $P = 36.2$ N.

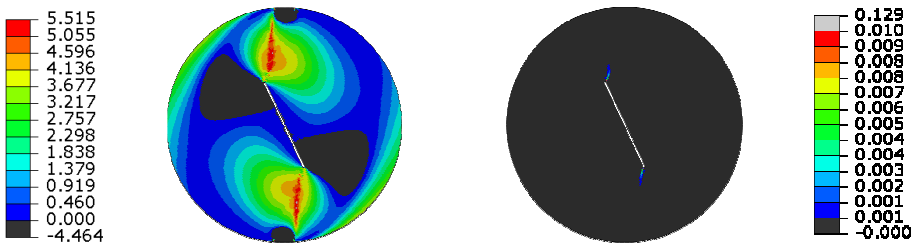


Fig. 4.9. Calculated maximum principal stress [MPa] and inelastic strain [-] fields with equivalent vertical compressive load for $a/R = 0.4$ and $\alpha = 25^\circ$, $P = 36.2$ N.

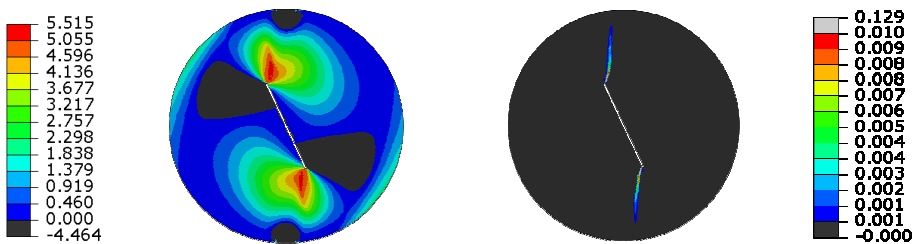


Fig. 4.10. Calculated maximum principal stress [MPa] and inelastic strain [-] fields with equivalent vertical compressive load for $a/R = 0.4$ and $\alpha = 25^\circ$, $P = 36.2$ N.

Table 4.5. Overview of measured and calculated fracture forces for $a/R = 0.4$.

α [°]	0	5	10	15	25.2
Calculated force [N/mm]	562.85	543.72	540.90	522.54	505.40
Thickness B [mm]	30.92	31.44	30.77	30.97	31.17
Force – Calculated FEA [kN]	17.40	17.10	16.70	16.18	15.80
Force P_C – Experiment [kN]	15.80	19.60	20.00	13.70	15.80

From Table 4.5 it can be noted, that the numerical analysis showed a reasonable agreement (difference up to 20%) for the $a/R = 0.267$ specimens and a good agreement (difference limited to 7%) for the $a/R = 0.4$ specimens.

A comparison of measured and calculated maximum forces for various notch inclination angles α can be found in Fig. 4.11.

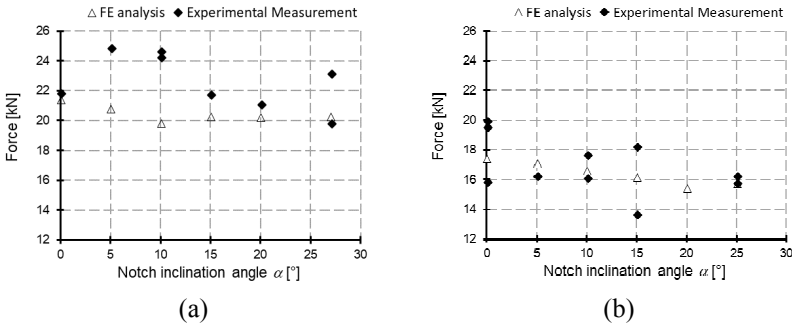


Fig. 4.11. A comparison of measured and calculated maximum forces for BDNC made from C 50/60 with thickness $B \approx 30$ mm: (a) $a/R = 0.267$ and (b) $a/R = 0.4$.

A typical numerical result from the simulation is a Load-displacement diagram, where a reaction load (N per unit width) is plotted against the total vertical displacement.

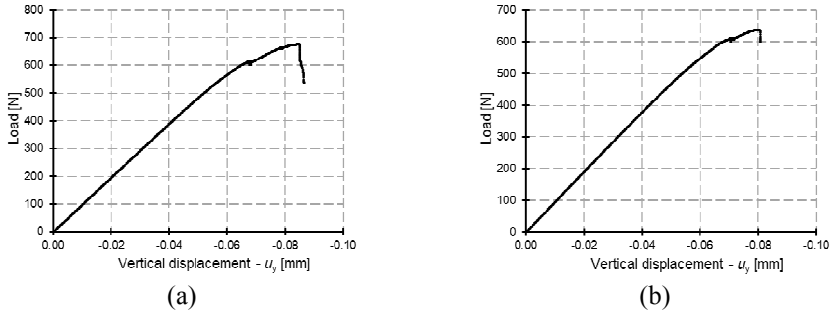


Fig. 4.12. Load-displacement diagram for BDNC made from C 50/60 with thickness $B \approx 30$ mm: $a/R = 0.267$ and for angle $\alpha = 0^\circ$ (a) and $\alpha = 25^\circ$ (b).

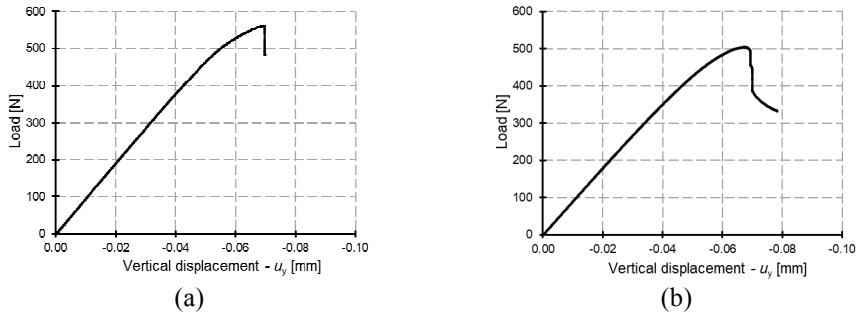


Fig. 4.13. Load-displacement diagram for BDNC made from C 50/60 with thickness $B \approx 30$ mm: $a/R = 0.4$ and for angle $\alpha = 0^\circ$ (a) and $\alpha = 25^\circ$ (b).

3.5 Conclusions

The C 50/60 concrete material was analysed in combination of experimental and numerical studies. From experimental campaign the fracture mechanical parameters of C 50/60 were evaluated by using Brazilian disc test specimen with a central notch. Numerical model of the BDCN provides information about failure behaviour of such a test. From the presented results above a following conclusion can be done:

- Fracture resistance curves for mixed mode I/II provide information about onset of fracture and help to predict failure.
- Fit of resistance curves depends on the T -stress and on critical distance r_C , which was in C 50/60 calculated for plane strain $r_C = 1.559$ mm and should not be neglected in the evaluation of the mixed mode fracture resistance.

- The numerical model provides accurate results of the crack pattern in studied BDCN geometry.
- The numerical results of maximum reaction loads give accurate results for used concrete damaged plasticity material model with an error limited to 4% for $a/R = 0.4$ and 20% for $a/R = 0.267$.

Acknowledgment

This paper has been written with financial support from the projects: FAST-J-18-5164, FAST-S-18-5614 and “National Sustainability Programme I” project “AdMaS UP – Advanced Materials, Structures and Technologies” (No. LO1408) supported by the Ministry of Education, Youth and Sports of the Czech Republic and Brno University of Technology.

The second author is Brno Ph.D. Talent Scholarship Holder – Funded by the Brno City Municipality.

References

- Abaqus, (2016), ‘Analysis User’s Manual 6.14’, *Dassault Systemes Simulia Corp., Providence*.
- Anderson, T.L. (2017) ‘Fracture mechanics: fundamentals and applications’, *CRC press*.
- Ayatollahi, M.R. and Aliha, M.R.M. (2008) ‘On the use of Brazilian disc specimen for calculating mixed mode I-II fracture toughness of rock materials’, *Engineering Fracture Mechanics*, 75 pp. 4631-4641, doi: 10.1016/j.engfracmech.2008.06.01.
- de Freitas, V. P. *et. al* (2013) ‘Durability of Building Materials and Components’, Springer Berlin Heidelberg.
- Erdogan, F. And Sih, G.C.(1963) ‘On the Crack Extension in Plates Under Plane Loading and Transverse Shear’, *Journal of Basic Engineering*, 85 pp. 519-525, doi: 10.1115/1.3656897.
- Fett, T (2001) ‘Stress intensity factors and T-stress for internally cracked circular disks under various boundary conditions’, *Engineering Fracture Mechanics*, 68 (2001) 1119-1136, doi: 10.1016/S0013-7944(01)00025-X
- Flager, F.L. (2003) ‘The design of building structures for improved life-cycle performance’.
- International Federation for Structural Concrete, (2010), ‘Model Code 2010, First complete draft’, Lausanne, Switzerland.
- Karihaloo, B.L. (1995) ‘Fracture Mechanics and Structural Concrete (Concrete Design and Construction Series)’, *Ed. Longman Scientific & Technical*. United States.

- Kmiecik, P. And Kamiński, M. (2011) 'Modelling of reinforced concrete structures and composite structures with concrete strength degradation taken into consideration', *Archives of Civil and Mechanical Engineering*, 11 pp. 623-636. doi: 10.1016/S1644-9665(12)60105-8.
- Lee, J. and Fenves Gregory. L. (1998) 'Plastic-Damage Model for Cyclic Loading of Concrete Structures', *Journal of Engineering Mechanics*, 124 pp. 892-900. doi: 10.1061/(ASCE)0733-9399(1998)124:8(892)
- Lubliner, J. et. al (1989) 'A plastic-damage model for concrete', *International Journal of Solids and Structures*, 25 pp. 299-326. Doi: 0.1016/0020-7683(89)90050-4.
- Miarka, P. et. al (2018) 'Comparison of Fracture Resistance of the Normal and High Strength Concrete Evaluated by Brazilian Disc Test', *Proceedings* (2), p. 399; doi:10.3390/ICEM18-05236.
- Miarka, P. et. al (2018a) 'Numerical Analysis of the Failure Behavior of a C50/60 Brazilian Disc Test Specimen with a Central Notch'. *Advances in Fracture and Damage Mechanics XVII. Key Engineering Materials*, 774, pp. 570-575. ISBN: 978-3-0357-1350-3. ISSN: 1662-9795, doi: 10.4028/www.scientific.net/KEM.774.570.
- Nawy, E.G. (2001) 'Fundamentals of High-Performance Concrete', Wiley, 2001.
- EN 12350-5 (2009), 'Testing fresh concrete, in: Part 5: Flow table test', *European Committee for Standardization*.
- Seitl, S. et al. (2018) 'The mixed-mode fracture resistance of C 50/60 and its suitability for use in precast elements as determined by the Brazilian disc test and three-point bending specimens', *Theoretical and Applied Fracture mechanics*, 97(3), pp. 108-119, doi: 10.1016/j.tafmec.2018.08.003.
- Tomek, R. (2017) 'Advantages of Precast Concrete in Highway Infrastructure Construction', *Procedia Engineering*, 196, pp. 176–180, doi: 10.1016/j.proeng.2017.07.188.
- Zimmermann, T. and Lehký, D. (2015) 'Fracture parameters of concrete C40/50 and C50/60 determined by experimental testing and numerical simulation via inverse analysis', *International Journal of Fracture*, (192), pp. 179–189, doi: 10.1007/s10704-015-9998-0.
- Williams, M.L. (1956) 'On the Stress Distribution at the Base of a Stationary Crack', *Journal of Applied Mechanics*, 24.
- Smith, D.J. et. al (2001), 'The role of T-stress in brittle fracture for linear elastic materials under mixed-mode loading', *Fatigue & Fracture of Engineering Materials & Structures*, 24 pp. 137-150. doi: 10.1046/j.1460-2695.2001.00377.x.